IOPscience iopscience.iop.org

Home Search Collections Journals About Contact us My IOPscience

Valence-band discontinuity at the C_{60}/Si(111)-7 × 7 interface

This article has been downloaded from IOPscience. Please scroll down to see the full text article.

1999 J. Phys.: Condens. Matter 11 L111

(http://iopscience.iop.org/0953-8984/11/13/002)

View the table of contents for this issue, or go to the journal homepage for more

Download details:
IP Address: 171.66.16.214
The article was downloaded on 15/05/2010 at 07:16

Please note that terms and conditions apply.

J. Phys.: Condens. Matter **11** (1999) L111–L118. Printed in the UK PII: S0953-8984(99)01877-9

LETTER TO THE EDITOR

Valence-band discontinuity at the C_{60}/Si(111)-7 × 7 interface

O Janzen† and W Mönch

Laboratorium für Festkörperphysik, Gerhard-Mercator-Universität Duisburg, D-47048 Duisburg, Germany

Received 16 February 1999

Abstract. The growth of fullerene films on Si(111)-7 × 7 surfaces and the formation of the C_{60}/Si(111)-7 × 7 interface was studied using low-energy electron diffraction, Auger electron spectroscopy and x-ray as well as ultraviolet photoemission spectroscopy. The initial growth of C_{60} proceeds layer-by-layer. No chemical reactions or interdiffusion were observed. The C_{60} deposition does not change the binding energies of Si(2p) and C(1s) electrons. Therefore, the band bending of the clean Si(111)-7 × 7 surface remains the same, irrespective of the C_{60} coverage. The photoemission measurements yield a valence-band discontinuity of 0.6 ± 0.2 eV at the C_{60}/Si(111)-7 × 7 interface. The band line-up at semiconductor interfaces is explained by the adjustment of the branch points in the continuum of the interface-induced gap states. Our experimentally observed valence-band offset agrees well with the theoretical predictions if the branch point of C_{60} is assumed at midgap position.

1. Introduction

Solid C_{60} is a new form of carbon crystal. At room-temperature C_{60} molecules are arranged in a face-centred cubic (fcc) structure with a lattice parameter of 14.198 Å [1]. The C_{60} molecules interact by van der Waals-force only. Saito *et al* [2] found solid C_{60} to have a semiconducting character with a direct band gap. Therefore, C_{60} films, deposited on Si, form semiconductor heterostructures. The electronic properties of such heterostructures are determined by the band-structure alignment across the interface. Essential parameters are the offsets of the valence- and the conduction-band edges.

Extensive experimental studies have been reported on the adsorption of C_{60} molecules and the growth of crystalline C_{60} films on Si(111) substrates. Techniques used were scanning-tunnelling microscopy (STM) [3–9], high-resolution electron energy-loss spectroscopy (HREELS) [10, 11], x-ray diffraction [12] and photoemission spectroscopy [13, 14]. Only two studies focused on the band-edge discontinuities at C_{60}/Si(111) interfaces [15, 16]. However, contradicting results were reported. Transport measurements yielded a valence-band discontinuity smaller than 0.42 eV [15], whereas photoemission gave a negative valence-band offset of −0.4 eV [16]. A negative offset means that the Si valence-band maximum is below the one of C_{60}. Unfortunately, no theoretical prediction of the valence-band offset at C_{60}/Si(111) interfaces is available.

In our present study, we determined the valence-band discontinuity at the C_{60}/Si(111) interfaces using x-ray and ultraviolet photoemission spectroscopy (XPS, UPS). We carefully controlled surface cleanliness and structure, and evaporated C_{60} onto well-ordered 7 × 7-reconstructed surfaces. This reconstruction is preserved beneath C_{60} films [12]. Our

† E-mail address: oliver_janzen@uni-duisburg.de.

 © 1999 IOP Publishing Ltd

measurements give a valence-band offset of 0.6±0.2 eV. We explain this experimental result by the continuum of interface-induced gap states (IFIGS), a concept that was successfully applied to explain the band line-up at interfaces between conventional semiconductors [17, 18].

2. Experimental details

The experiments were carried out in a stainless-steel ultrahigh vacuum (UHV) system, which consists of a rapid load-lock, a preparation chamber and an analysis chamber. The rapid load-lock was used for transferring the samples into the UHV and reached a pressure of less than 10^{-4} Pa within 10 min. In the preparation chamber samples could be heated by electron bombardment from the back. The analysis chamber was equipped with a low-energy electron diffraction (LEED) optics and a cylindrical mirror analyser, having an integral electron gun for Auger electron spectroscopy (AES). Furthermore, an x-ray source with a Zr/Mg double anode and a differentially pumped, window-less discharge lamp were employed for x-ray and ultraviolet photoemission spectroscopy (XPS, UPS), respectively. Energy distribution curves of photoemitted electrons were measured with a concentric hemispherical analyser. Both the analysis and the preparation chamber had base pressures of approximately 10^{-8} Pa.

Samples, cut from n-type Si(111) wafers, were first oxidized in 1 bar of O_2 at 900 °C for 30 min, then dipped into hydrofluoric acid, which was diluted by a buffered $HF:NH_4F:NH_4OH$-solution, and eventually transferred into the UHV system. This *ex situ* preparation resulted in H-terminated Si(111):H-1 × 1 surfaces. Hydrogen was then desorbed by heating the samples indirectly to 850 °C for about 2 min. After this procedure, no contaminants were detected by AES or XPS, sharp 7 × 7 LEED patterns with low background were observed and the UPS spectra showed the surface states of the 7 × 7 reconstruction. As usual, AES spectra were recorded as first derivatives and intensities of the lines were taken as the peak-to-peak heights (PPH) of the Auger signals.

Pure C_{60} (Hoechst AG, 'super gold grade' $> 99.9\%$) was evaporated from a Knudsen cell in the analysis chamber. It was carefully outgassed at 400 °C for more than 24 h. During exposures, its temperature was held at approximately 300 °C and the background pressure was lower than 2×10^{-8} Pa. The growth rate at this temperature was determined as 0.5 monolayers (ML) per minute. Here, a monolayer is defined by the results of our AES measurements and is described in the next section.

3. Results

Figure 1 shows the variation of the Si(LVV) and C(KLL) intensities as a function of the C_{60} deposition time. Here, the PPHs of the lines were normalized by their maximum values, i.e., the PPHs of the Si(LVV) line recorded with the clean substrate and of the C(KLL) line recorded after 600 s deposition of C_{60}, respectively. Each data point represents an average of measurements at three different spots on the sample. The error bars are within the symbol size. The dashed lines are meant to guide the eye.

The variations of the Si(LVV) and C(KLL) intensities as a function of deposition time may be described by a sequence of straight line segments. The kinks then indicate the completion of continuous layers, i.e., after 120 s and 240 s of deposition time the first and the second C_{60} monolayer, respectively, are completed. The initial growth thus proceeds layer-by-layer [19]. This yields a growth rate of 0.5 ML per minute or 0.4 nm per minute since the distance between two (111) layers of C_{60} is approximately 0.8 nm [1]. Initially, a sharp 7 × 7 LEED pattern was observed. Each C_{60} exposure slightly increased the diffuse background, but the

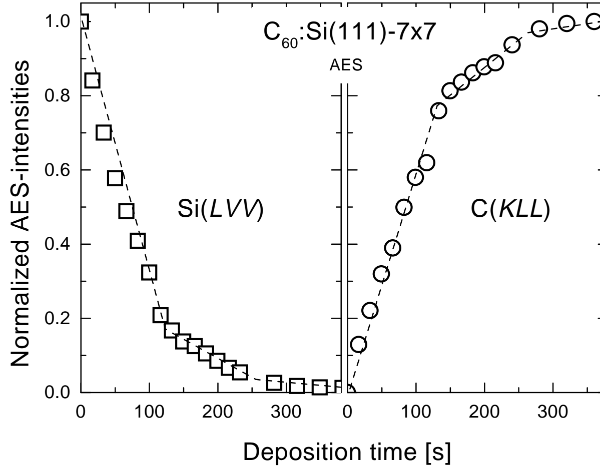

Figure 1. AES intensity ratios Si(LVV)/Si(LVV)$_0$ and C(KLL)/C(KLL)$_\infty$ recorded with a Si(111)-7 × 7 sample as a function of the C_{60} deposition time. The dashed lines are meant to guide the eye.

7 × 7 spots remained sharp up to approximately 120 s of deposition time. Thereafter, the background became so intense that the 7 × 7 pattern could no longer be recognized.

Previous investigations demonstrated that C_{60} multilayers desorb during annealing at 400 °C [5, 9], but one monolayer of C_{60} remains adsorbed on Si(111)-7 × 7 surfaces. STM observations [8] identified this monolayer to consist of seven C_{60} molecules per 7 × 7 surface unit-mesh which is equivalent to 1.12×10^{14} C_{60} molecules per cm^2. The Si(LVV)/C(KLL) PPH-ratio is 0.75 ± 0.05 after 120 s of deposition but amounts to 0.85 ± 0.05 if the C_{60} monolayer is prepared by the annealing of a film of 5 ML at 400 °C for 10 min. The difference in the Si(LVV)/C(KLL) intensity ratios indicates that the area density of the C_{60} molecules in the as-deposited monolayer is slightly below the one after multilayer desorption. This may be due to adsorbate ordering at elevated temperatures. In the following, we take these AES measurements as calibration of the growth rate and quote C_{60} coverages either in monolayers or in nanometers.

The escape depths λ_{Si} and λ_C of 90 eV Si(LVV) and 270 eV C(KLL) Auger electrons, respectively, may be determined from the experimental data shown in figure 1. As a function of the number n of complete C_{60} monolayers, Beer's law gives the substrate and the overlayer intensities as

$$I_{Si}(n) = I_{Si}^0 \exp(-n d_{111} \varsigma_{Si}) \tag{1}$$

and

$$I_C(n) = I_C^\infty [1 - \exp(-n d_{111} \varsigma_C)] \tag{2}$$

respectively, where I_{Si}^0 is the Si(LVV) intensity measured with the clean Si(111) substrate and I_C^∞ is the C(KLL) signal recorded with a C_{60} film, the thickness of which exceeds a few escape lengths λ_C. The thickness of a complete C_{60} layer is taken as the (111) interlayer distance $d_{111} = 0.82$ nm in solid fcc-C_{60}. The attenuation parameters

$$\varsigma_{Si,C} = 1/\lambda_p + 1/(\lambda_{Si,C} \cos \alpha_{CMA}) \tag{3}$$

are determined by the penetration length $\lambda_p = 4.2$ nm of the primary 3 keV electrons and the acceptance angle $\alpha_{CMA} \approx 42°$ of the CMA. The ratios $I_{Si,C}(1)/I_{Si,C}(2)$ of the intensities at

the corresponding kinks in figure 1 then give the escape lengths $\lambda_{Si} = 0.67 \pm 0.05$ nm and $\lambda_C = 0.85 \pm 0.05$ nm. These values are close to what has been reported for *conventional* semiconductors [17].

Figure 2 displays Si(2p) and C(1s) XPS signals recorded with a clean Si(111)-7 $\times$ 7 surface and after its coverage with up to five monolayers of C_{60}. The binding energies are referenced to the Fermi level which was recorded with a 200 nm thick Pb film. Since the main C(1s) line, measured with the thickest C_{60} film, will consist of one component only, its full width at half maximum of 0.9 ± 0.05 eV represents the overall resolution determined by the Mg(Kα) line and the analyser. The Si(2p) line consists of two spin-orbit split components which cannot be resolved. With increasing C_{60} coverage, this peak decreases in intensity and it has almost vanished after deposition of 5 ML. However, its peak shape and, even more importantly, its energy position does not change as a function of C_{60} coverage. The latter observation means that the band bending at the clean Si(111)-7 $\times$ 7 surface is preserved beneath the C_{60} film, probably due to the persistence of the 7 $\times$ 7 structure itself [12]. The C(1s) signal becomes more intense with increasing coverage. The spectrum recorded with the 5 ML thick film exhibits the satellite features that are typical of C_{60} [20]. The structures 2–6 are due to energy losses of photoemitted electrons that excite π–π^* transitions. Specifically, feature 2 has been attributed to a shakeup process involving direct excitations between states derived from the highest occupied molecular orbitals (HOMO) and from the lowest unoccupied molecular orbitals (LUMO). If we neglect correlation effects the energy shift of this satellite with respect to the main line gives the band gap $W_g^{C_{60}}$ of solid C_{60} as 1.8 ± 0.1 eV. The binding energy of the main peak, 1, of the C(1s) signal with regard to the Fermi level is the same for all C_{60} coverages.

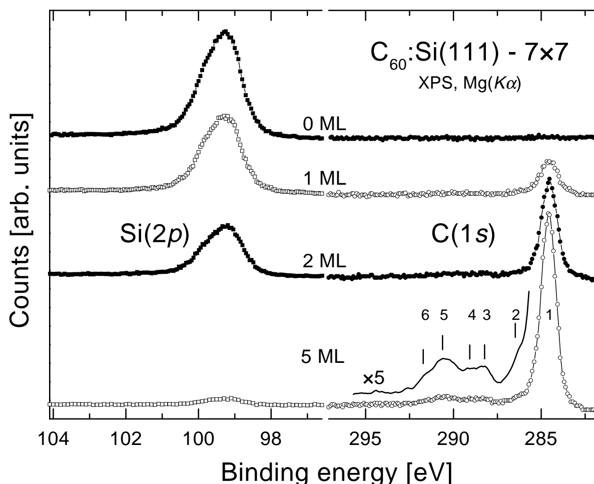

Figure 2. XPS spectra of Si(2p) and C(1s) core levels of a clean and subsequently C_{60}-covered Si(111)-7 $\times$ 7 surface. Binding energies are referenced to the Fermi level. The solid line in the bottom spectrum on the right represents a smoothed magnification of the C(1s) satellites. The features labelled 2–6 represent energy losses of photoemitted electrons caused by π–π^* transitions.

Figure 3 displays valence-band spectra of the clean 7 $\times$ 7 surface and a 16.5 nm thick C_{60} film excited with HeI radiation. The binding energies are again referenced to the experimentally determined Fermi level. The structures labelled S_1, S_2 and S_3 in the top spectrum are due to emission from surface states of the 7 $\times$ 7 surface which were identified as the dangling bonds of adatoms (S_1) and of rest-atoms (S_2) and backbonds of the adatoms

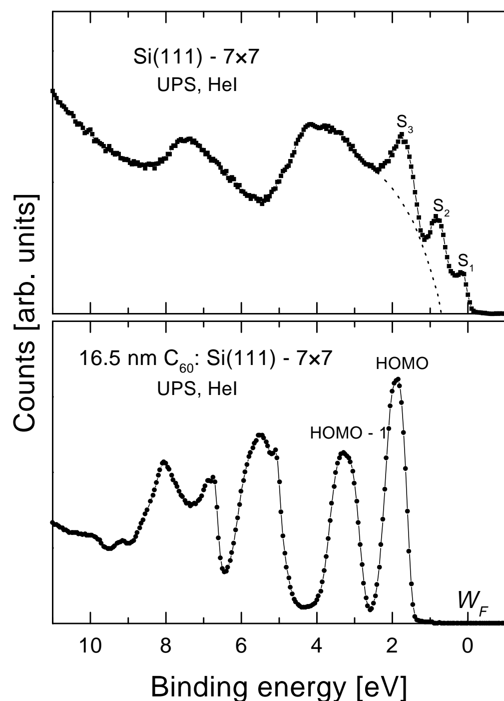

Figure 3. Valence band spectra of a clean Si(111)-7 × 7 surface and a 16.5 nm thick C_{60} film. The structures labelled S_1, S_2 and S_3 are due to emission from surface states of the 7 × 7-reconstructed surface. The dashed line indicates the contribution from the valence-band top. The bottom spectrum displays the valence bands of C_{60} where the structure labelled HOMO is derived from the highest occupied molecular orbital.

(S_3) [17]. The dashed line represents the contribution of the valence-band top to the total emission. The onset energy $W_F - W_{vs}^{Si}$ of the valence-band emission may be determined from the well-known energy differences $W_{vs}^{Si} - W(S_2) = 0.15 \pm 0.05$ eV of the surface state S_2 and $W_{vs}^{Si} - W(Si(2p_{3/2})) = 98.56 \pm 0.05$ eV of the Si($2p_{3/2}$) core level [21] to the valence-band top W_{vs}. Our experimental data $[W_F - W(S_2)]_{\text{exp}} = 0.85 \pm 0.05$ eV and $[W_F - W(Si(2p_{3/2}))]_{\text{exp}} = 99.25 \pm 0.05$ eV both give $W_F - W_{vs}^{Si} = 0.7 \pm 0.1$ eV. This value concurs with the observation reported earlier [17] that the surface states of the Si(111)-7 × 7 surface pin the Fermi level at 0.7 eV above the valence-band maximum.

The spectrum recorded with a 16.5 nm thick C_{60} film on a Si(111)-7 × 7 surface shows the sequence of peaked features typical of C_{60} [20]. These structures are derived from the molecular orbitals and their sharpness indicates the weak interactions between the molecules. By linear extrapolation of the high-energy tail of the HOMO-derived structure we obtain the valence-band maximum W_v^{C60} of the C_{60} film at 1.3 ± 0.05 eV below the Fermi level. Considering this value and the binding energy $W_F - W(C(1s)) = 284.6 \pm 0.1$ eV we determine the binding energy $W_v - W(C(1s))$ of the C(1s) core levels with regard to the valence-band maximum as 283.3 ± 0.1 eV in solid fcc-C_{60}.

4. Discussion

The C_{60}/Si(111)-7 × 7 interface is abrupt since no chemical reaction occurs and the initial growth proceeds in a layer-by-layer mode. Layer-plus-islands growth has been reported earlier

[5] but we have no indications for islands. This may be due to different growth conditions. At abrupt interfaces the band line-up is established within a few Ångströms and is described by band-edge offsets. The XPS data displayed in figure 2 reveal that the binding energies of both the Si(2p) and the C(1s) levels with regard to the Fermi level do not vary with increasing thickness of the C_{60} film. On the silicon side of the C_{60}/Si(111)-7 × 7 interface, the pinning of the Fermi level or, in other words, the interface band-bending thus remains the same irrespective of the C_{60} depositions. On the other side, even a thickness of 16.5 nm is not sufficient for the formation of a space-charge layer in the C_{60} film. Therefore, the valence-band offset in C_{60}/Si(111)-7 × 7 heterostructures equals the difference of the binding energies of the valence-band maxima with regard to the Fermi level. They were determined from the XPS and the UPS spectra displayed in figures 2 and 3 as $W_F - W_{vs}^{Si} = 0.7 \pm 0.1$ eV and $W_F - W_{vs}^{C60} = 1.3 \pm 0.05$ eV so that we obtain

$$\Delta W_v = W_{vi}^{Si} - W_{vi}^{C60} = W_F - W_{vs}^{C60} - (W_F - W_{vs}^{Si}) 0.6 \pm 0.2 \text{ [eV]}. \tag{4}$$

Within the limits of experimental error, this valence-band offset agrees with the value obtained from transport measurements at C_{60}/Si(111):H-1 × 1 heterostructures [15]. However, our photoemission data do not confirm a negative valence-band offset [16].

Figure 4 displays schematically the band diagram of C_{60}/Si(111)-7 × 7 heterostructures. Neither the value nor the sign of the conduction-band discontinuity ΔW_c can be reliably determined from the above experimental value of the valence-band offset. This is due to the large scatter of the band-gap widths reported for solid C_{60} that range from 1.3 eV up to 2.3 eV [20–25]. For an estimate of the conduction-band offset, we take the band gap energy W_g^{C60} as 1.8 eV. This is an average of the experimental values obtained from photoconductance measurements and electron energy-loss as well as photoemission spectroscopy. This value also

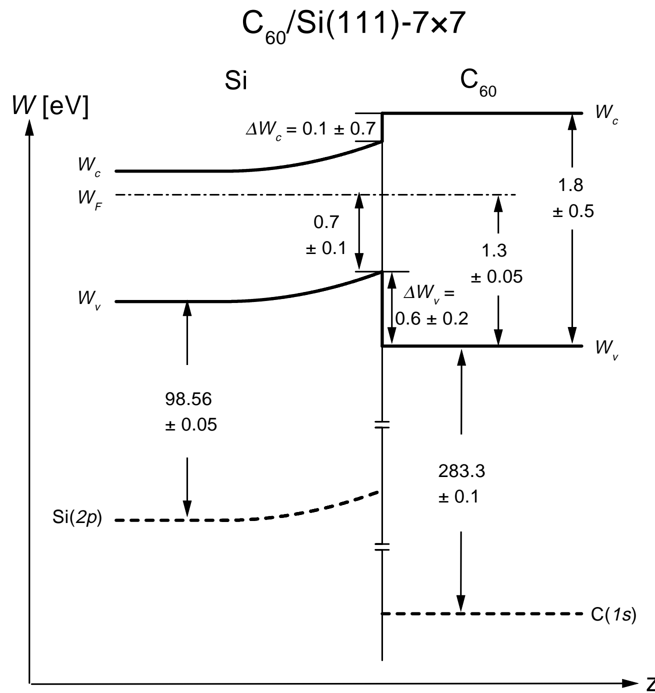

Figure 4. Energy band diagram of the C_{60}/Si(111)-7 × 7 interface.

equals the energy loss observed with the C(1s) photoelectrons in figure 2, that was attributed to HOMO–LUMO transitions. We then estimate a conduction-band offset of 0.1 eV, as indicated in figure 4.

The line-up of the electronic band structures at ideal semiconductor interfaces is determined by the continuum of interface-induced gap states (IFIGS) [17, 18]. These intrinsic interface states originate from the wavefunction tails in the energy range where the valence or the conduction band of one semiconductor overlaps the band gap of the other one. The IFIG states derive from the virtual gap states (ViGS) of the complex band structure of semiconductors. Their character changes across the band gap from predominantly acceptor-like close to the bottom of the conduction band, to mainly donor-like close to the valence-band maximum. The energy W_{bp}, at which the dominant proportion changes, is called their branch point. Again, the branch-point energy is an intrinsic property of each semiconductor. Provided no charge transfer occurs at a semiconductor heterostructure then the bands line up such that the branch points of the two semiconductors in contact are at the same energy. Partially ionic interface bonds, on the other hand, will add an additional layer of interface dipoles and the voltage drop across this electric double layer contributes another term to the band offsets. Chemically speaking, the corresponding charge transfer may be described by the difference $X_2 - X_1$ in the electronegativities of the semiconductors in contact. The valence-band discontinuity may then be written as [26]

$$\Delta W_v^{IFIGS} = (W_{bp} - W_v)_2 - (W_{bp} - W_v)_1 + D(X_2 - X_1) = \Phi_{bp}^2 - \Phi_{bp}^1 + D(\Delta X) \qquad (5)$$

where $D(\Delta X)$ represents the interface dipoles.

The branch points W_{bp} of the tetrahedrally coordinated semiconductors are close to the middle of the dielectric or average band gap at the mean value point of the Brillouin zone [18]. The branch-point energy of solid C_{60}, on the other hand, was not calculated but it may be estimated. Due to the weak interaction between the C_{60} molecules the HOMO- and LUMO-derived bands of solid C_{60} only slightly disperse so that the band gap varies by less than 0.5 eV along the high-symmetry directions of the Brillouin zone [2, 27, 28]. If we completely ignore any dispersion of the C_{60} energy bands and assume a constant band-gap width of 1.8 eV across the whole Brillouin zone we then estimate the energy position of the C_{60} branch point at 0.9 eV above the valence-band maximum. We further neglect the dipole term $D(X_{C60} - X_{Si})$. Using the branch-point energy $\Phi_{bp}^{Si} = (W_{bp} - W_v)_{Si} = 0.36$ eV calculated by Tersoff [29] for silicon, we finally obtain the valence-band offset at C_{60}/Si heterostructures as

$$\Delta W_V^{C60/Si} \approx W_g^{C60}/2 - \Phi_{bp}^{Si} = 0.54 \text{ [eV]}.$$

This value agrees remarkably well with the experimentally observed valence-band offset of 0.6 ± 0.2 eV.

5. Conclusions

To summarize, the present study investigated the formation of the C_{60}/Si(111)-7 × 7 interface and the alignment of the electronic band structure at this interface. During the deposition of the C_{60} molecules no chemical reactions occured and the 7 × 7 reconstruction was preserved beneath the C_{60} film. Up to at least two monolayers, the initial growth proceeded layer-by-layer. The interface was abrupt and the band bending of the clean Si(111)-7 × 7 surface remained unchanged. The offset $\Delta W_v^{C60/Si} = W_v^{C60} - W_v^{si}$ of the valence-band maxima at the interface was determined as 0.6 ± 0.2 eV. This experimental value is explained by the continuum of interface-induced gap states. When the slight energy dispersion of the C_{60} HOMO and

LUMO bands is ignored, the IFIGS model yields a valence-band discontinuity of 0.54 eV at C_{60}/Si(111)-7 × 7 interfaces, in good agreement with the experimental data.

The authors would like to thank Dr W Appel from Hoechst AG for providing the 'super gold grade' C_{60} powder.

References

[1] Dresselhaus M S, Dresselhaus G and Eklund P C 1996 *Science of Fullerenes and Carbon Nanotubes* (San Diego: Academic)
[2] Saito S and Oshiyama A 1991 *Phys. Rev. Lett.* **66** 2637
[3] Li Y Z, Chander M, Patrin J C, Weaver J H, Chibante L P F and Smalley R E 1992 *Phys. Rev.* B **45** 13 837
[4] Wang X-D, Hashizume T, Shinohara H, Saito Y, Nishina Y and Sakurai T 1992 *Japan. J. Appl. Phys.* **31** L983
Sakurai T, Wang X-D, Hashizume T, Nishina Y, Shinohara H and Saito Y 1993 *Appl. Surf. Sci.* **67** 281
[5] Xu H, Chen D M and Creager W N 1993 *Phys. Rev. Lett.* **70** 1850
[6] Balooch M and Hamza A V 1993 *Appl. Phys. Lett.* **63** 150
[7] Chen D M, Xu H, Creager W N and Burnett P 1994 *J. Vac. Sci. Technol.* B **12** 1910
[8] Chen D and Sarid D 1994 *Phys. Rev.* B **49** 7612
Chen D, Chen J and Sarid D 1994 *Phys. Rev. B* **50** 10 905
[9] Dunn A W, Moriarty P, Upward M D and Beton P H 1996 *Appl. Phys. Lett.* **69** 506
[10] Suto S, Kasuya A, Ikeno O, Hu C-W, Wawro A, Nishitani R, Goto T and Nishina Y 1996 *Japan. J. Appl. Phys.* **33** L1489
Suto S, Sakamoto K, Wakita T, Harada M and Kasuya A 1998 *Surf. Sci.* **402–404** 523
[11] Dumas P, Gruyters M, Rudolf P, He Y, Yu L-M, Gensterblum G, Caudano R and Chabal Y J 1996 *Surf. Sci.* **368** 330
[12] Hong H, McMahon W E, Zschack P, Lin D-S, Aburano R D, Chen H and Chiang T-C 1992 *Appl. Phys. Lett.* **61** 3127
[13] Moriarty P, Upward M D, Dunn A W, Ma Y-R, Beton P H and Teehan D 1998 *Phys. Rev.* B **57** 362
[14] Sakamoto K, Harada M, Kondo D, Kimura A, Kakizaki A and Suto S 1998 *Phys. Rev.* B **58** 13951
[15] Chen K M, Jia Y Q, Jin S X, Wu K, Zhao W B, Li C Y, Gu Z N and Zhou X H 1995 *J. Phys.: Condens. Matter* **7** L201
[16] Zhu J-S, Liu X-M, Xu S-H, Wu J-X and Sun X-F 1996 *Solid State Commun.* **98** 417
[17] Mönch W 1995 *Semiconductor Surfaces and Interfaces* 2nd edn (Berlin: Springer), and references therein
[18] Mönch W 1998 *Appl. Phys. Lett.* **72** 1899
Mönch W 1997 *Appl. Surf. Sci.* **117/118** 380
Mönch W 1996 *J. Appl. Phys.* **80** 5076
[19] Lüth H 1993 *Surfaces and Interfaces of Solids* 2nd edn (Berlin: Springer)
[20] Weaver J H, Martins J L, Komeda T, Chen Y, Ohno T R, Kroll G H, Troullier N, Haufler R E and Smalley R E 1991 *Phys. Rev. Lett.* **66** 1741
[21] Miyazaki S, Schäfer J, Ristein J and Ley L 1996 *Appl. Phys. Lett.* **68** 1247
[22] Faiman D, Goren S, Katz E A, Koltun M, Melnik N, Shames A and Shtutina S 1997 *Thin Solid Films* **295** 283
[23] Ren S L, Wang Y, Rao A M, McRae E, Holden J M, Hager T, Wang K, Lee W-T, Ni H F, Selegue J and Eklund P C 1991 *Appl. Phys. Lett.* **59** 2678
[24] Hansen P L, Fallon P J and Krätschmer W 1991 *Chem. Phys. Lett.* **181** 367
[25] Hosoya M, Ichimura K, Wang Z H, Dresselhaus G, Dresselhaus M S and Eklund P C 1994 *Phys. Rev. B* **49** 4981
[26] Tejedor S and Flores F 1978 *J. Phys. C: Solid State Phys.* **11** L19
[27] Weaver J H and Poirier D M 1994 *Solid State Phys.* **48** ed Ehrenreich H and Spaepen F (San Diego: Academic) p 1
[28] Troullier N and Martins J L 1992 *Phys. Rev.* B **46** 1754
[29] Tersoff J 1984 *Phys. Rev. Lett.* **52** 465